JOC The Journal of Organic Chemistry

Article

pubs.acs.org/joc

Reversible Hydrolysis Reaction with the Spore Photoproduct under Alkaline Conditions

Surya Adhikari,[†,§] Gengjie Lin,[†,§] and Lei Li*[,†,‡]

[†]Department of Chemistry and Chemical Biology, Indiana University−Purdue University Indianapolis (IUPUI), 402 North Blackford Street, Indianapolis, Indiana, 46202, United States

[‡]Department of Biochemistry and Molecular Biology & Department of Dermatology, Indiana University School of Medicine, Indianapolis, Indiana 46202, United States

Supporting Information

ABSTRACT: DNA lesions may reduce the electron density at the nucleobases, making them prone to further modifications upon the alkaline treatment. The dominant DNA photolesion found in UV-irradiated bacterial endospores is a thymine dimer, 5-thyminyl-5,6-dihydrothymine, i.e., the spore photoproduct (SP). Here we report a stepwise addition/elimination reaction in the SP hydrolysis product under strong basic conditions where a ureido group is added to the carboxyl moiety to form a cyclic amide, regenerating SP after eliminating a hydroxide ion. Direct amidation of carboxylic acids by reaction with amines in the presence of a catalyst is well documented; however, it is very rare for an amidation reaction to occur without activation. This uncatalyzed SP reverse reaction in aqueous solution is even more surprising because the carboxyl moiety is not a good electrophile due to the negative charge it carries. Examination of the base-catalyzed hydrolyses of two other saturated pyrimidine lesions, 5,6-dihydro-2′-deoxyuridine and pyrimidine (6−4) pyrimidone photoproduct, reveals that neither reaction is reversible even though all three hydrolysis reactions may share the same *gem*-diol intermediate. Therefore, the SP structure where the two thymine residues maintain a stacked conformation likely provides the needed framework enabling this highly unusual carboxyl addition/elimination reaction.

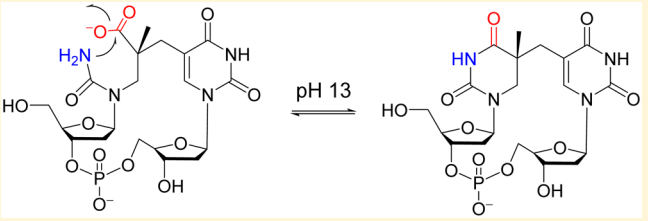

INTRODUCTION

As the repository of genetic information in living cells, the integrity and stability of DNA are essential to life. However, DNA is under constant environmental assault resulting in various DNA damages.[1,2] The best-known example is the formation of pyrimidine dimers after exposure to the UV portion of sunlight.[3,4] Other environmental factors such as tobacco smoke are known to induce DNA lesions too.[5] Besides environmental agents, DNA is subject to oxidative damage from byproducts of metabolism, resulting in lesions such as 8-oxo-7,8-dihydro-2′-deoxyguanosine (8-oxo-dG).[6,7] These damages, if not repaired in time, are prone to inducing mutations during polymerase bypass events,[8,9] the accumulation of which may eventually lead to human diseases like cancer and aging. Being able to selectively detect DNA lesions as potential biomarkers via either footprinting or sequencing analysis is of interest.[10] To achieve this goal, better understandings of the chemical properties of DNA lesions are required.

Detection of nucleotide modifications can be achieved after chemical or biochemical treatments. For instance, the different reactions between sodium bisulfite and cytosine or 5-hydroxymethylcytosine (5hmC) allow the sequencing assay for 5hmC, an important epigenetic marker.[11] The hydroxyl group in 5-hmC can be linked to a glucose under the catalysis of T4-β-glucosyltransferase, which then allows the 5-hmC sequencing after further modifications at the glucose.[12] Further, chemical treatment with a carbodiimide derivative converts the carboxyl group of 5-carboxylcytosine (5caC) to an amide, which is stable under the bisulfite treatment, subsequently enabling 5caC sequencing.[13] Taking advantage of the unique properties/reactions of the abasic site[14,15] or 8-oxo-dG,[16] assays enabling analysis of these lesions may also be developed. Modification of nucleobase generally reduces the electron density at the ring.[1] Alkaline treatments can be used for lesion differentiation because intact nucleobases are relatively stable while the less electron-rich modified nucleobases may lead to strand scissions under basic conditions.[1] Hence, the alkaline lability reflects the essential properties of DNA lesions and may be used for damage analysis. Indeed, the pyrimidine (6−4) pyrimidone photoproduct (6−4PP) results in strand cleavage upon base treatments,[17] which was used to analyze its formation sites in the genome.[18]

Despite the fact that the alkaline liability has been utilized in lesion analysis for a long time, the detailed mechanism behind the lability of a given DNA lesion remains largely unclear. In bacterial endospores, a special thymine dimer named 5-thyminyl-5,6-dihydrothymine, i.e., the spore photoproduct (SP), is generated as the dominant DNA photolesion.[19−24] This lesion accumulates in dormant spores and is repaired

Received: July 29, 2016
Published: August 18, 2016

DOI: 10.1021/acs.joc.6b01846
J. Org. Chem. 2016, 81, 8570−8576

Scheme 1. Formation of SP Hydrate via a *gem*-Diol Intermediate

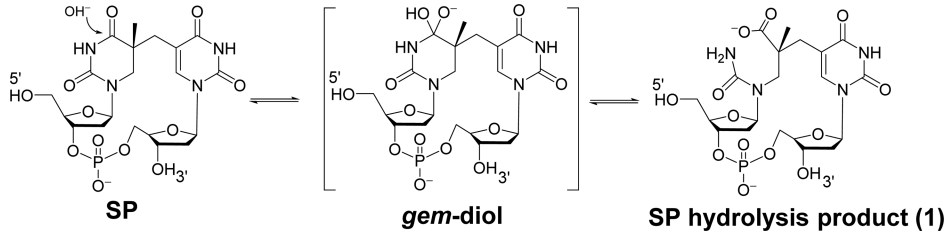

rapidly mainly by the spore photoproduct lyase in germinating and outgrowing spores.[25−31] Recently, our group found that the alkaline treatment of SP leads to the rupture of the N3−C4 bond at the saturated 5′-pyrimidine ring to yield the corresponding hydrolysis product **1** (Scheme 1).[32] Similar reactions were observed in the hydrolyses of 5,6-dihydro-2′-deoxyuridine (dHdU)[32] and 6−4PP[33] upon alkaline treatments, indicating that such a N3−C4 bond cleavage is likely a common feature possessed by a saturated pyrimidine ring.[32]

Using ^{18}O-labeled water, we demonstrated that the rupture of the N3−C4 bond proceeds via a *gem*-diol intermediate after the hydroxide addition to the C4═O moiety; the resulting **1** contains a deprotonated carboxylate moiety carrying a negative charge in 0.2 M KOH (Scheme 1). The charge reduces the electron deficiency at the carboxyl group, making it a poor electrophile. Thus, it is difficult for the carboxyl moiety to undergo a nucleophilic addition followed by hydroxide elimination reaction, regenerating the pyrimidine ring. Indeed, the hydrolyses of dHdU[32] and 6−4PP[33,34] are irreversible, supporting this assumption. However, the SP hydrolysis in ^{18}O-labeled water led to one ^{18}O incorporation into **1** at the first 30 min of the reaction. This singly labeled species gradually disappeared upon prolonged incubation, which was accompanied by the incorporation of one ^{18}O label into SP and two ^{18}O atoms into **1**. Such an observation implies that the alkaline-catalyzed SP hydrolysis reaction is likely reversible as shown in Scheme 1; however, the possibility that the second ^{18}O incorporation into **1** is carried out via a similar *gem*-diol intermediate at the carboxyl group of **1** cannot be excluded.[32] Although direct amidation of carboxylic acids by reacting with amines in the presence of catalysts has been extensively studied,[35−37] amide formation without activation of reactants as indicated in the possible reverse reaction of the SP hydrolysis is extremely rare. To confirm that the reverse process indeed occurs, we examined the reaction in detail.

RESULTS AND DISCUSSION

We first repeated the SP hydrolysis reaction by incubation of dinucleotide SP TpT in 0.2 M KOH at ambient temperature. The reaction leads to the formation of **1** (Figure 1A), the yield of which increased in the first 8 h and remained constant thereafter indicating the realization of equilibrium. Because **1** is unstable after isolation and rapidly decays at neutral pH,[32] it is difficult for us to quantify it by HPLC. Hence, we relied on the reduction of the SP signal in the HPLC chromatogram for our calculation of the conversion yield. We found that at 25 °C when the reaction completes a **1**/SP ratio of 2.1 is reached.

A previous study reacted 6−4PP with 50 mM KOD in D_2O at 60 °C inside an NMR tube.[33] Such a condition converted about 90% of 6−4PP to the corresponding hydration product, allowing its characterization by NMR spectroscopy.[33] Since we cannot stabilize **1** for a prolonged period of time as it tends to

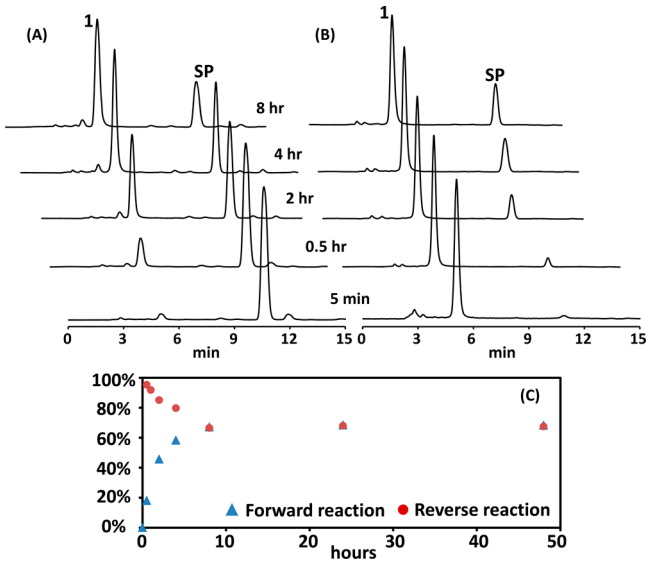

Figure 1. (A) HPLC chromatograms showing the SP → **1** conversion with 0.2 M of KOH at ambient temperature. (B) HPLC chromatograms showing the **1** → SP conversion under 0.2 M of KOH at ambient temperature. (C) Percentage of **1** found in the forward reaction (SP → **1**) and the reverse reaction (**1** → SP) at various time points.

either isomerize or revert back to SP,[32] we chose to treat SP under basic conditions to generate a SP/**1** mixture. Because the NMR spectrum of SP is well established,[38,39] useful information can be obtained via analysis of the mixture signals.

The reaction was conducted in 0.2 M KOD at ambient temperature for 24 h. As shown in Figure 2, during the course of the reaction, some of the ^{1}H NMR signals from SP kept decreasing while new signals due to the formation of **1** gradually increased. The signal changes appeared to stop after 8 h, consistent with our HPLC analysis above. Although we were unable to assign all ^{1}H NMR signals for **1** in the final ^{1}H NMR spectra, it is obvious that the largest chemical shift changes occur at the 5′-nucleoside, especially from H_{6a}, $H_{1A'}$, and $H_{4A'}$. Further, a new singlet signal at 7.32 ppm gradually increased during the treatment. This signal is close to the singlet peak of H_{6b} of SP at 7.36 ppm and is thus ascribed to the H_{6b} of **1**. Integration of these two signals allows us to determine the **1**/SP ratio to be 2.1, which again agrees with the ratio determined by HPLC. Thus, we conclude that in the presence of 0.2 M KOH the forward reaction exhibits a pseudoequilibrium constant K_{eq} of 2.1.[40]

If the reaction is reversible, we should be able to start from **1** and generate SP under the same basic conditions. We therefore isolated **1** by HPLC from the SP hydrolysis reaction, desalted, and redissolved it in 0.2 M KOH. Monitoring the reaction by HPLC shows that the SP peak indeed gradually increased

DOI: 10.1021/acs.joc.6b01846
J. Org. Chem. 2016, 81, 8570−8576

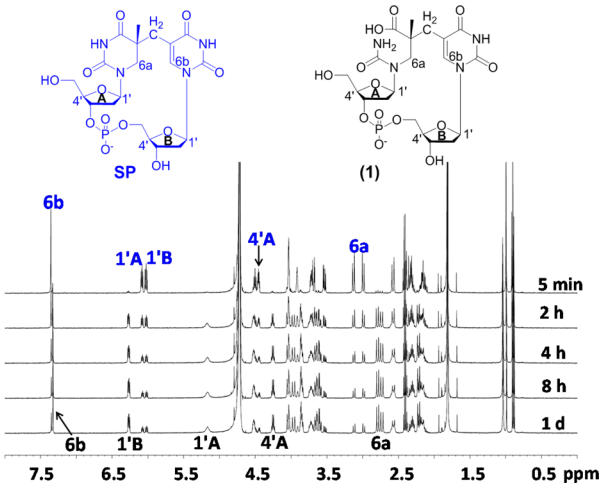

Figure 2. NMR spectra showing the SP → **1** conversion with 0.2 M of KOD in D_2O at ambient temperature. Based on the signal integration of H**6b** for SP TpT and **1**, the SP/**1** ratio was determined to be 1:2.1 after the reaction reaches equilibrium. Although it is impossible for us to assign every signal belonging to **1** in the reaction mixture, it is obvious that the largest chemical shift changes from those of SP were observed at the saturated 5′-nucleoside on which the hydrolysis reaction occurs.

during the course of the reaction (Figure 1B). The ratio of **1**/SP was stabilized after 8 h again at 2.1 (Figure 1C), fully supporting our assumption that the carboxyl moiety in **1** is attacked by the ureido group leading to the *gem*-diol intermediate that then eliminates a hydroxide ion to close the ring, resulting in SP.

Elevated temperatures are often used in DNA-footprinting studies. After revealing the SP hydrolysis reaction at ambient temperature, we next investigated the impact of temperature to the generation of **1** in 0.2 M KOH. Similar to the 6–4PP reaction,[33,34] the SP → **1** conversion is much faster at a higher temperature, reaching equilibrium within 0.5 h at 90 °C. The yield of **1**, however, is lower (Figure 3A and the SI). At 90 °C, the yield was found to be 43 ± 1%, contrasting to the 68 ± 1% at 25 °C. Moreover, the yield increases to 78 ± 1% at 4 °C, although it takes ∼4 days for the reaction to reach equilibrium.

The ratio between **1** and SP remains at 2.1 if we allow the reaction to complete at 4 °C, transfer it to room temperature, and let the system re-equilibrate, again implying the reversible nature of the SP hydrolysis reaction. These observations also suggest that at a higher temperature, although the conversion to **1** is faster, the reaction is thermodynamically unfavorable. The reverse reaction was examined similarly; the **1**/SP ratio was found to be the same as that obtained in the forward reaction at a given temperature.[40]

Using the pseudoequilibrium constants K_{eq} determined with 0.2 M KOH at various temperatures, we plotted $\ln(K_{eq})$ against $1/T$ according to the Van't Hoff equation (eq 1) as shown in Figure 4A.

$$\ln(K_{eq}) = -\frac{\Delta H}{RT} + \frac{\Delta S}{R} \quad (1)$$

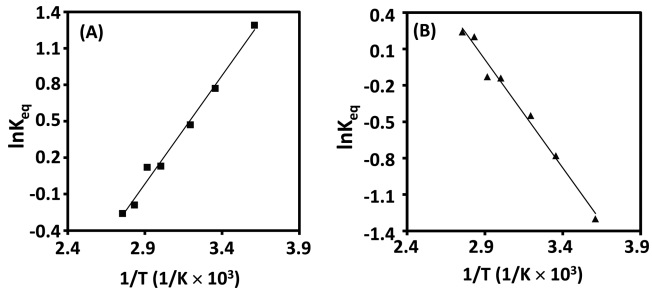

Figure 4. (A) Van't Hoff plot of the SP hydrolysis reaction under 0.2 M KOH. (B) Van't Hoff plot of the reverse reaction leading to the formation of SP in 0.2 M KOH. Same ΔH and ΔS but with opposite signs were deduced from the forward and the reverse reactions.

The plot allows us to determine ΔH to be −14.87 ± 1.5 kJ mol^{-1} and ΔS to be −43.24 ± 3 J mol^{-1} K^{-1} for the SP hydration reaction. The negative value of ΔH indicates that the SP → **1** conversion is exothermic under strong basic conditions; the negative ΔS reflects the fact that the SP hydrolysis is an addition reaction combining two molecules (OH^- and SP) to a larger product **1** and the system becomes more ordered after the reaction. Both ΔH and ΔS carry a negative sign, implying that the ring-opening reaction to

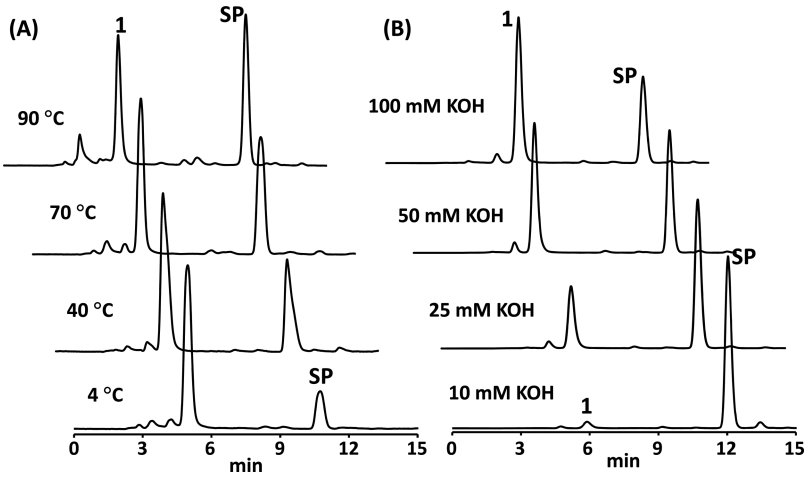

Figure 3. (A) HPLC chromatograms showing the SP → **1** conversion in 0.2 M of KOH at selective temperatures after the reactions reach equilibrium. (B) HPLC chromatograms showing the SP → **1** conversion under various concentrations of KOH at the ambient temperature after the reactions reach equilibrium. Detailed information on these reactions is available in the SI.

DOI: 10.1021/acs.joc.6b01846
J. Org. Chem. 2016, 81, 8570–8576

Scheme 2. Mechanism for SP-Induced Strand Scission after the Hot Base Treatment

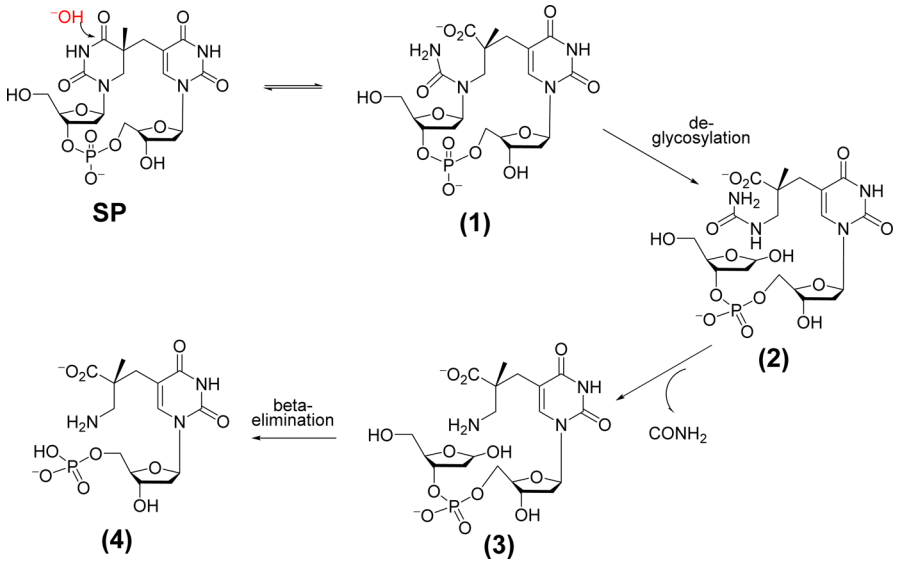

produce **1** is favored by a low temperature. We also conducted the Van't Hoff plot for the reverse reaction (Figure 4B), which results in ΔH of 14.84 ± 1.5 kJ mol^{-1} and ΔS of 43.15 ± 3 J mol^{-1} K^{-1}. As expected for any truly reversible reactions, these parameters, within the experimental error, are the same as those obtained from the forward reaction except carrying opposite signs. Taken together, our data imply that *the SP/**1** equilibrium favors SP at an elevated temperature*.

As shown above, the SP hydrolysis reaction is driven by strong basic conditions. Compared with the submillimolar SP, the 0.2 M KOH was present in large excess. The KOH concentration change during the reaction can be ignored, leading to the pseudo-first-order reaction analyzed above. We next examined the reaction under various KOH concentrations. In 0.2 M KOH, about 68% of SP is converted to **1** at room temperature. At a lower KOH concentration, the yield is also lower. At pH 12 (100 mM KOH), the yield of **1** is 62 ± 1%. At pH 11, it is only 4 ± 0.5% after a 4-day incubation (Figure 3B). The formation of **1** cannot be reliably observed by our HPLC assay when the KOH concentration becomes even lower, although the *gem*-diol intermediate is still formed as suggested by our previous ^{18}O-labeling studies.[32]

Lesion-induced strand scission after hot alkaline treatments is typically used for DNA-footprinting studies. After revealing the detailed chemical properties of **1**, we next examined how this knowledge may help us understand the DNA strand cleavage reaction at **1** mediated by piperidine. Hot piperidine treatment employing 1 M piperidine at 90 °C for 30 min is a typical assay used in the field.[1] A 1 M piperidine solution possesses a pH of 12.5. At 25 °C, we found that treatment by 1 M piperidine converts ∼35% SP to **1** when the reaction reaches the equilibrium.[40] At 90 °C, the yield decreases to 6%,[40] much lower than the ∼43% found in 0.2 M KOH at the same temperature. Further, the 30 min hot piperidine treatment only resulted in negligible strand cleavage (<1%),[40] suggesting that SP cannot be labeled as a "piperidine-labile" lesion.

As shown previously, a 30 min treatment by 0.2 M KOH at 90 °C resulted in significant strand scission.[32] Thus, the lack of strand scission during the hot piperidine treatment must be owing to the reduced basicity. As shown in Scheme 2, the SP-induced strand cleavage contains two processes: the reversible formation of **1** and the irreversible deglycosylation reaction from **1** that triggers a cascade of reactions eventually leading to strand scission.[32] The deglycosylation step is likely facilitated by the formation of a Schiff base intermediate at the glycosidic bond of the 5′-thymine residue of **1**, similar to what was observed in the hydrolysis of dHdU.[41] The formation of the strand cleave product **4** is reached via metastable intermediates **2** and **3**; all three species were isolated by HPLC and characterized by mass spectrometry as shown in our previous studies.[32] Therefore, the irreversible nature of the second process determines that the yield of the strand cleavage reaction is controlled by the concentration of **1**. The negative ΔH and ΔS exhibited by the SP → **1** conversion determine a lower yield of **1** at a higher temperature. Thus, the efficiency of hot alkaline treatments for SP-induced strand scission is determined by the combined effect of two opposite trends: a faster reaction rate but a less favorable equilibrium at a high temperature. To compensate for this negative impact, stronger basic conditions producing more **1** and consequently more irreversible deglycosylation reaction have to be adopted.

Direct amidation of carboxylic acids by reaction with amines[35−37] and *N*,*N*′-dimethylurea[42] has been extensively studied. Moreover, amide formation between alkali metal carboxylate salts and amines was also described.[43] These reactions were conducted in organic solvents with the involving molecules activated by using various catalysts. Amide formation in cyclic constrained systems is also found during the ring-closure reaction in the formation of inosine monophosphate (IMP) from 5-formaminoimidazole-4-carboxamide ribonucleotide (FAICAR) in purine biosynthesis.[44] This reaction involves a neutral aldehyde instead of a less active carboxyl moiety and is catalyzed by IMP synthase. In contrast, the SP formation from a negatively charged carboxylate via the reversible hydrolysis process occurs without any reactant activation. Moreover, among all of the cases studied to date, it is the only established example of a reaction under a true equilibrium.

The unique property of SP reported here likely results from its unique chemical structure. To date, the base-catalyzed acyl addition/elimination reaction has been studied in four pyrimidine lesions: 6−4PP, SP, CPD, and dHdU. Although the first step, i.e., formation of the *gem*-diol intermediate at

DOI: 10.1021/acs.joc.6b01846
J. Org. Chem. 2016, 81, 8570−8576

Scheme 3. Mechanisms for the Base-Catalyzed Hydrolyses of Other Saturated Pyrimidine Lesions

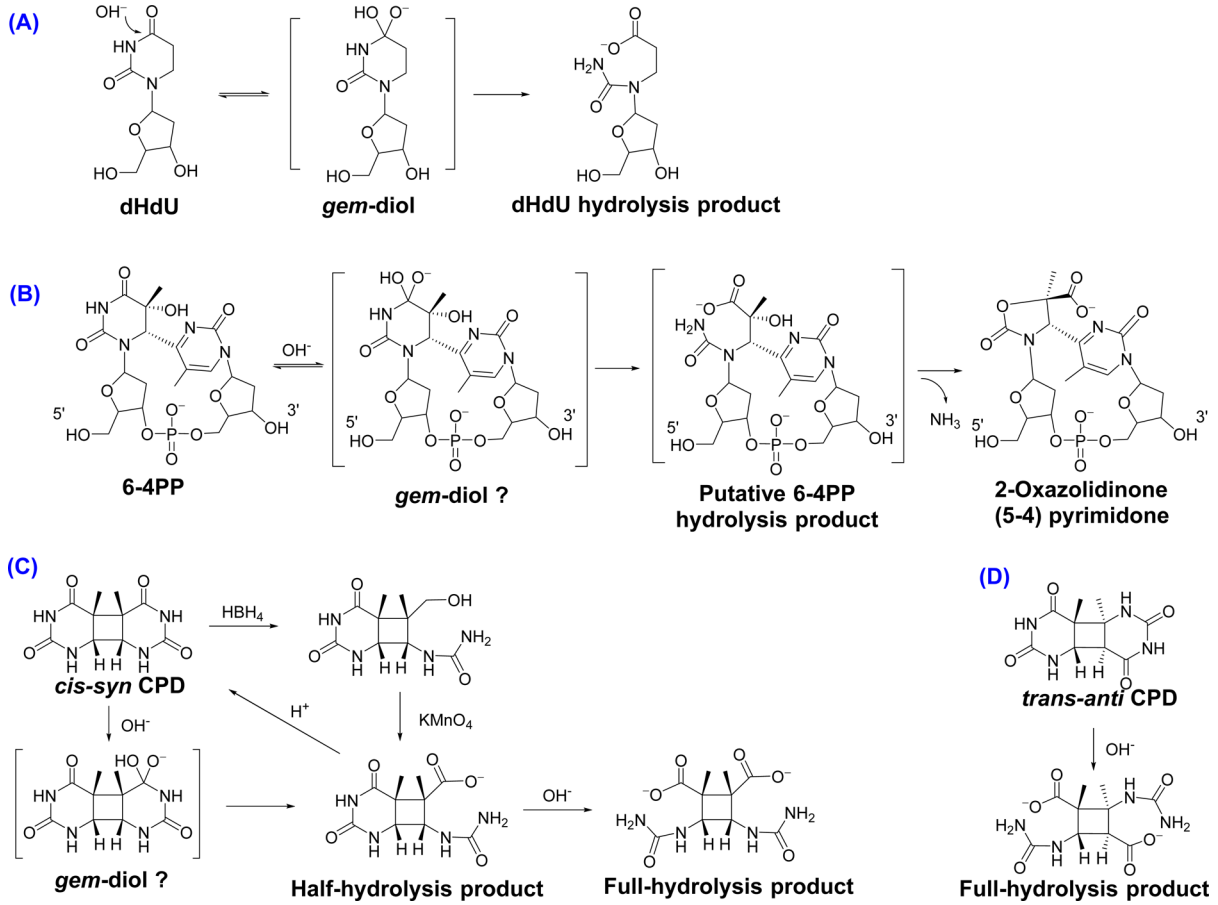

C4═O followed by rupture of the N3−C4 bond, probably occurs for all lesions, the resulting hydrolysis products exhibit very distinctive chemical properties. The N3−C4 bond rupture from the *gem*-diol intermediate in dHdU is irreversible (Scheme 3A); the resulting hydrolysis product has few other choices but undergoes the deglycosylation process eventually leading to strand cleavage as shown in our previous work.[32] In contrast, the SP hydrolysis reaction is reversible, which lowers the yield of **1** and decreases the strand scission efficiency. Similar to dHdU, the 6−4PP hydrolysis is unlikely reversible after the formation of the *gem-diol* intermediate (Scheme 3B). As shown in our previous work, the putative 6−4PP hydrolysis product is not stable enough to be isolated; what can be isolated is the deamination product 2-oxazolidinone (5−4) pyrimidone.[34] Therefore, even if the direct hydrolysis process is reversible, the presence of the 5-OH group in the putative 6−4PP hydrolysis product should be able to effectively compete with the reverse reaction, leading to 2-oxazolidinone (5−4) pyrimidone to lock up the product.[34]

The CPD hydrolysis represents another interesting system. Via UV irradiation of the thymine base, both *cis-syn* and *trans-syn* CPDs were generated. The alkaline treatment of the *trans-syn* CPD readily broke the two N3−C4 bonds, resulting in the full-hydrolysis product (Scheme 3D).[45] In contrast, probably due to the maintained stacking interactions between the two thymine ring, the *cis-syn* CPD was considered as being unable to support the hydrolysis product formation upon hot alkaline treatment by the initial study.[45] A later study, however, found that a 24-h treatment using 0.1 M NaOH at 75 °C did result in the full-hydrolysis product as shown in Scheme 3C.[46] However, there was no attempt to reveal whether such a hydrolysis reaction is reversible as observed in the SP reaction here. Interestingly, upon $NaBH_4$ treatment, the *cis-syn* CPD can be converted to a half-hydrolysis product with the resulting carboxyl moiety being reduced to an alcohol (Scheme 3C). It is likely that the alcohol formation stabilizes the product, preventing the reverse reaction from occurring. After oxidizing the alcohol by potassium permanganate, the resulting carboxyl moiety can then react with the ureido group under acidic conditions, regenerating the *cis-syn* CPD.[45]

Thus, the chemical structure of a given pyrimidine lesion largely determines its chemical property upon base treatment, i.e., its alkaline liability. Between dHdU and SP, although they share similar structures, the cross-link bond between the two thymine bases in SP likely places some restriction on the 3D structure, which provides the framework driving the occurrence of the reverse reaction, even though the negatively charged carboxyl moiety is a weak electrophile and the amide is a weak nucleophile. Both SP and *cis-syn* CPD largely maintain the stacking interaction between the two thymine residues as revealed by the dinucleotide[47,48] as well as the lesion-containing oligonucleotide structures.[49−51] Based on what we have learned about the SP hydrolysis here, it is likely that the *cis-syn* CPD may also exhibit a similar reversible hydrolysis reaction; such a hypothesis awaits further test in the future.

DOI: 10.1021/acs.joc.6b01846
J. Org. Chem. 2016, 81, 8570−8576

CONCLUSION

In conclusion, we here report a very rare example of uncatalyzed direct amidation of a carboxylate by reacting with the ureido moiety in the reverse reaction of the SP hydrolysis under strong basic conditions. The fact that only SP but not dHdU or 6−4PP exhibits this reactivity indicates that the chemical structures of various DNA lesions play important roles in determining their reactivity. Such a property is important to our effort in lesion characterization, chemical synthesis, or investigation of the consequences of their persistence in a genome. Moreover, the understanding of the distinctive chemical properties of SP or other pyrimidine damages may enable targeted lesion analysis and searching for biomarkers in the genome by using DNA footprinting or sequencing techniques, which are being actively pursued in our laboratory.

EXPERIMENTAL SECTION

Materials and Methods. All reagents and chemicals were purchased from commercial vendors and used without further purification. All reactions were carried out using oven- or flame-dried glassware under an argon atmosphere in freshly distilled solvents. The ^{1}H NMR spectra were obtained on a 500 MHz NMR Fourier transform spectrometer in deuterium oxide (D_2O) with residual H_2O as the standard. The chemical shifts in NMR spectra were reported in parts per million (ppm). High-resolution MS and tandem mass spectrometry (MS/MS) analyses were performed using a LC-Q-TOF MS spectrometer and the MS data analyzed via the associated software.

Synthesis of Dinucleotide SP TpT- and SP-Containing Oligonucleotides. The dinucleotide SP TpT was synthesized using a procedure originally developed by Kim et al.[52] and later modified by our group.[39] The SP-containing oligonucleotide 5′-TT(SP)T-3′ was synthesized via the SP phosphoramidite prepared by our group[53] and standard automated solid phase DNA synthesis procedures as described in our previous publication.[32]

HPLC Product Analyses. HPLC analyses were performed at room temperature using a HPLC system coupled to a UV/vis detector at 268 nm. An Agilent ZORBAX Bonus-RP column (5 μm particle size, 250 × 4.6 mm i.d.) was equilibrated in the mobile phase A (10 mM ammonium acetate in 99% water and 1% acetonitrile, pH 6.5), and compounds were eluted with an ascending gradient (1−10%) of acetonitrile in 20 min at a flow rate of 1 mL/min. Products were confirmed by LC/MS spectrometry.

Formation of 1 in 0.2 M KOH. Dinucleotide SP TpT was dissolved in 0.2 M KOH to a final concentration of 0.75 mM. The resulting solution was maintained at room temperature (25 °C) to allow the formation of **1** until the reaction equilibrium was attained as assessed by monitoring 1 μL aliquots of the reaction mixture by HPLC. Under such conditions, the reaction equilibrium was reached in about 8 h. The maximum yield of **1** was 68 ± 1% upon attainment of equilibrium (Figure S1).

Formation of 1 in 0.2 M KOH at Various Temperatures. Dinucleotide SP TpT was dissolved in 0.2 M KOH to a final concentration of 0.75 mM. The resulting solution (100 μL) was transferred to a 1.5 mL Eppendorf tube. Mineral oil (20 μL) was added to prevent water evaporation, and the tube was then placed on an aluminum heating block maintained at various temperatures. At various time points, 2 μL of solution was taken out and mixed with 8 μL 100 mM ammonium acetate to reduce the basicity of the solution right before HPLC analysis (Figure S2). The reaction also produces a fragmentation product **2** (Scheme 2) as revealed by LC/MS analysis as shown in our previous work.[32]

Formation of 1 at Various pH Values. Various concentrations of KOH were employed in this study. Namely: 400 mM KOH (pH 13.6); 200 mM KOH (pH 13.3); 100 mM KOH (pH 13); 50 mM KOH (pH 12.7); and 25 mM KOH (pH 12.4); and 10 mM KOH (pH 12). SP TpT was dissolved in these KOH solutions to a final concentration of 0.75 mM. The resulting solutions were maintained at ambient temperature for 48−96 h to allow the reactions to achieve equilibrium, as confirmed by the HPLC analyses of 1 μL aliquots of solution extracted (Figure S3).

Preparation of 1. Dinucleotide SP TpT was dissolved in 0.2 M KOH to a final concentration of 0.75 mM. The resulting solution was maintained at room temperature (25 °C) for a day until the reaction equilibrium was attained. About 40 μL of the reaction mixture was mixed with 40 μL of 100 mM ammonium acetate to reduce the solution basicity, and the formed **1** was purified by HPLC as described above. A 1 mL fraction of the desired product was collected in an Eppendorf tube containing 20 μL of 20 mM KOH to create a basic environment to stabilize **1**. This collected fraction was concentrated to nearly about 40 μL followed by desalting. Desalting was done by the reversed-phase HPLC with a UV/vis detector at 268 nm and a Waters XBridge Oligonucleotide BEH C18 column (2.5 μm, 4.6 × 50 mm). The column was equilibrated with 99% mobile phase A (water) and 1% of mobile phase B (acetonitrile). The pure compound was eluted with an ascending gradient (1−10% in 20 min) of mobile phase B. The compound eluant (1 mL) was mixed with 20 μL of 10 mM KOH to maintain a basic solution and stabilize the isolated compound **1**. The resulting solution was then concentrated to about 100 μL under high vacuum at 0 °C.

Formation of SP TpT from 1 in 0.2 M KOH. The purified compound **1** was then mixed with 2 M KOH in a 1:9 ratio to ensure the final concentration of KOH to be 0.2 M. The solution was maintained at room temperature for 2 days to allow the **1** → SP reverse reaction to occur and the reaction equilibrium to be reached. The equilibrium was attained in about 8 h as assessed by HPLC analysis. The maximum yield of SP was found to be ∼32% upon attainment of equilibrium (Figure S4).

Formation of SP TpT from 1 in 0.2 M KOH at Various Temperatures. The desalted **1** was mixed with 2 M KOH under a 1:9 ratio to reach a final KOH concentration of 0.2 M. The resulting solution (100 μL) was transferred to a 1.5 mL Eppendorf tube. Mineral oil (20 μL) was added to form a mineral oil layer on the top to prevent water evaporation, and the tube was then placed on an aluminum heating block maintained at various temperatures. At various time points, 2 μL of solution was taken out, mixed with 8 μL 100 mM ammonium acetate, and immediately analyzed by HPLC (Figure S5).

Formation of 1 from SP TpT in 1 M Piperidine at Room Temperature. Dinucleotide SP TpT was dissolved in 1 M piperidine to a final concentration of 0.75 mM. The resulting solution (100 μL) was transferred to a 1.5 mL Eppendorf tube, and the reaction was carried out at room temperature for various periods of time. At different time points, 2 μL of solution was taken out and analyzed by HPLC after mixing with 8 μL of 100 mM ammonium acetate. The products revealed by HPLC were further confirmed by LC/MS (Figure S6).

SP TpT Hydration Reaction in 1 M Piperidine at 90 °C. Dinucleotide SP TpT was dissolved in 1 M piperidine solution to a final concentration of 0.75 mM. The resulting solution (100 μL) was transferred to a 1.5 mL Eppendorf tube. Mineral oil (20 μL) was added to form a mineral oil layer to prevent water evaporation, and the tube was then placed on an aluminum heating block maintained at 90 °C. After 30 min, 2 μL solution was taken out, mixed with 8 μL 100 mM ammonium acetate, and immediately analyzed by HPLC. Compound **1** was produced at ∼6% yield under this treatment. The reaction also produced <1% strand cleavage product **4** as analyzed by HPLC and confirmed by LC/MS.

SP TpT Hydration in a 5-mer Oligonucleotide in 1 M Piperidine at 90 °C. To confirm the results obtain in dinucleotide SP TpT reaction, we repeated the SP hydrolysis reaction using 5-mer oligonucleotide TTSPT in 1 M piperdine at 90 °C for 30 min. The reaction was analyzed using the HPLC method described in our previous work (Figure S8).[32] The yield of SP hydration product was determined to be around 2−4% under these conditions. Less than 0.5% of the oligonucleotide added underwent strand cleavage reaction as judged by HPLC peak integration.

DOI: 10.1021/acs.joc.6b01846
J. Org. Chem. 2016, 81, 8570−8576

■ ASSOCIATED CONTENT

Supporting Information

The Supporting Information is available free of charge on the ACS Publications website at DOI: 10.1021/acs.joc.6b01846.

HPLC chromatograms of the reactions (PDF)

■ AUTHOR INFORMATION

Corresponding Author

*E-mail: lilei@iupui.edu.

Author Contributions

§S.A. and G.L. contributed equally.

Notes

The authors declare no competing financial interest.

■ ACKNOWLEDGMENTS

We thank the National Institutes of Health (RES017177) and the National Science Foundation (CHE 1454184) for financial support. The NMR and MS facilities at IUPUI are supported by National Science Foundation MRI Grant Nos. CHE-0619254 and DBI-0821661, respectively.

■ REFERENCES

(1) Burrows, C. J.; Muller, J. G. *Chem. Rev.* **1998**, *98*, 1109.
(2) Pogozelski, W. K.; Tullius, T. D. *Chem. Rev.* **1998**, *98*, 1089.
(3) Improta, R.; Santoro, F.; Blancafort, L. *Chem. Rev.* **2016**, *116*, 3540.
(4) Ravanat, J. L.; Douki, T.; Cadet, J. *J. Photochem. Photobiol., B* **2001**, *63*, 88.
(5) Yuan, J.-M.; Butler, L. M.; Stepanov, I.; Hecht, S. S. *Cancer Res.* **2014**, *74*, 401.
(6) Cadet, J.; Douki, T.; Ravanat, J. L. *Free Radical Biol. Med.* **2010**, *49*, 9.
(7) Greenberg, M. M. *Acc. Chem. Res.* **2012**, *45*, 588.
(8) Yang, W. *Biochemistry* **2014**, *53*, 2793.
(9) Sharma, S.; Helchowski, C. M.; Canman, C. E. *Mutat. Res., Fundam. Mol. Mech. Mutagen.* **2013**, *743*−*744*, 97.
(10) Dedon, P. C.; DeMott, M. S.; Elmquist, C. E.; Prestwich, E. G.; McFaline, J. L.; Pang, B. *Biomarkers Med.* **2007**, *1*, 293.
(11) Booth, M. J.; Ost, T. W.; Beraldi, D.; Bell, N. M.; Branco, M. R.; Reik, W.; Balasubramanian, S. *Nat. Protoc.* **2013**, *8*, 1841.
(12) Song, C.-X.; Szulwach, K. E.; Fu, Y.; Dai, Q.; Yi, C.; Li, X.; Li, Y.; Chen, C.-H.; Zhang, W.; Jian, X.; Wang, J.; Zhang, L.; Looney, T. J.; Zhang, B.; Godley, L. A.; Hicks, L. M.; Lahn, B. T.; Jin, P.; He, C. *Nat. Biotechnol.* **2011**, *29*, 68.
(13) Lu, X.; Song, C.-X.; Szulwach, K.; Wang, Z.; Weidenbacher, P.; Jin, P.; He, C. *J. Am. Chem. Soc.* **2013**, *135*, 9315.
(14) Riedl, J.; Fleming, A. M.; Burrows, C. J. *J. Am. Chem. Soc.* **2016**, *138*, 491.
(15) Zhang, X.; Price, N. E.; Fang, X.; Yang, Z.; Gu, L.-Q.; Gates, K. S. *ACS Nano* **2015**, *9*, 11812.
(16) Hong, I. S.; Greenberg, M. M. *Bioorg. Med. Chem. Lett.* **2015**, *25*, 4918.
(17) Franklin, W. A.; Lo, K. M.; Haseltine, W. A. *J. Biol. Chem.* **1982**, *257*, 13535.
(18) Pfeifer, G. P.; Drouin, R.; Riggs, A. D.; Holmquist, G. P. *Proc. Natl. Acad. Sci. U. S. A.* **1991**, *88*, 1374.
(19) Setlow, P.; Li, L. *Photochem. Photobiol.* **2015**, *91*, 1263.
(20) Desnous, C. l.; Guillaume, D.; Clivio, P. *Chem. Rev.* **2010**, *110*, 1213.
(21) Setlow, P. *Annu. Rev. Microbiol.* **1995**, *49*, 29.
(22) Nicholson, W. L.; Munakata, N.; Horneck, G.; Melosh, H. J.; Setlow, P. *Microbiol. Mol. Biol. Rev.* **2000**, *64*, 548.
(23) Setlow, P. *J. Appl. Microbiol.* **2006**, *101*, 514.
(24) Setlow, P. *Trends Microbiol.* **2007**, *15*, 172.
(25) Yang, L.; Li, L. *J. Biol. Chem.* **2015**, *290*, 4003.
(26) Yang, L.; Nelson, R. S.; Benjdia, A.; Lin, G.; Telser, J.; Stoll, S.; Schlichting, I.; Li, L. *Biochemistry* **2013**, *52*, 3041.
(27) Yang, L.; Li, L. *Int. J. Mol. Sci.* **2013**, *14*, 13137.
(28) Yang, L.; Lin, G.; Nelson, R. S.; Jian, Y.; Telser, J.; Li, L. *Biochemistry* **2012**, *51*, 7173.
(29) Yang, L.; Lin, G.; Liu, D.; Dria, K. J.; Telser, J.; Li, L. *J. Am. Chem. Soc.* **2011**, *133*, 10434.
(30) Kneuttinger, A. C.; Kashiwazaki, G.; Prill, S.; Heil, K.; Müller, M.; Carell, T. *Photochem. Photobiol.* **2014**, *90*, 1.
(31) Broderick, J. B.; Duffus, B. R.; Duschene, K. S.; Shepard, E. M. *Chem. Rev.* **2014**, *114*, 4229.
(32) Lin, G.; Jian, Y.; Dria, K. J.; Long, E. C.; Li, L. *J. Am. Chem. Soc.* **2014**, *136*, 12938.
(33) Higurashi, M.; Ohtsuki, T.; Inase, A.; Kusumoto, R.; Masutani, C.; Hanaoka, F.; Iwai, S. *J. Biol. Chem.* **2003**, *278*, 51968.
(34) Lin, G.; Jian, Y.; Ouyang, H.; Li, L. *Org. Lett.* **2014**, *16*, 5076.
(35) Mohy El Dine, T.; Erb, W.; Berhault, Y.; Rouden, J.; Blanchet, J. *J. Org. Chem.* **2015**, *80*, 4532.
(36) Orliac, A.; Gomez Pardo, D.; Bombrun, A.; Cossy, J. *Org. Lett.* **2013**, *15*, 902.
(37) Lanigan, R. M.; Starkov, P.; Sheppard, T. D. *J. Org. Chem.* **2013**, *78*, 4512.
(38) Mantel, C.; Chandor, A.; Gasparutto, D.; Douki, T.; Atta, M.; Fontecave, M.; Bayle, P. A.; Mouesca, J. M.; Bardet, M. *J. Am. Chem. Soc.* **2008**, *130*, 16978.
(39) Lin, G.; Li, L. *Angew. Chem., Int. Ed.* **2010**, *49*, 9926.
(40) See the Supporting Information.
(41) Jian, Y.; Lin, G.; Chomicz, L.; Li, L. *J. Am. Chem. Soc.* **2015**, *137*, 3318.
(42) Talukdar, D.; Saikia, L.; Thakur, A. J. *Synlett* **2011**, *2011*, 1597.
(43) Goodreid, J. D.; Duspara, P. A.; Bosch, C.; Batey, R. A. *J. Org. Chem.* **2014**, *79*, 943.
(44) Zrenner, R.; Stitt, M.; Sonnewald, U.; Boldt, R. *Annu. Rev. Plant Biol.* **2006**, *57*, 805.
(45) Witkop, B.; Kunieda, T. *J. Am. Chem. Soc.* **1971**, *93*, 3493.
(46) Malone, M. E.; Pellowjarman, M. V.; Salter, L. F. *S Afr. J. Chem.* **1989**, *42*, 166.
(47) Cadet, J.; Voituriez, L.; Hruska, F. E.; Grand, A. *Biopolymers* **1985**, *24*, 897.
(48) Lin, G.; Chen, C.-H.; Pink, M.; Pu, J.; Li, L. *Chem. - Eur. J.* **2011**, *17*, 9658.
(49) Singh, I.; Lian, Y.; Li, L.; Georgiadis, M. M. *Acta Crystallogr., Sect. D: Biol. Crystallogr.* **2014**, *70*, 752.
(50) Park, H.; Zhang, K.; Ren, Y.; Nadji, S.; Sinha, N.; Taylor, J.-S.; Kang, C. *Proc. Natl. Acad. Sci. U. S. A.* **2002**, *99*, 15965.
(51) McAteer, K.; Jing, Y.; Kao, J.; Taylor, J. S.; Kennedy, M. A. *J. Mol. Biol.* **1998**, *282*, 1013.
(52) Kim, S. J.; Lester, C.; Begley, T. P. *J. Org. Chem.* **1995**, *60*, 6256.
(53) Jian, Y.; Li, L. *J. Org. Chem.* **2013**, *78*, 3021.

DOI: 10.1021/acs.joc.6b01846
J. Org. Chem. 2016, 81, 8570−8576